EVALUATING MARINE GAS-HYDRATE SYSTEMS PART II: ROCK-PHYSICS JOINT INVERSION OF ELECTRICAL RESISTIVITY AND SEISMIC VELOCITIES

DIANA SAVA, BOB HARDAGE, MIKE DeANGELO and PAUL MURPHY

Bureau of Economic Geology, Jackson School of Geosciences, The University of Texas at Austin, Austin, TX 78713, U.S.A. diana.sava@beg.utexas.edu

(Received June 12, 2010; revised version accepted January 28, 2011)

ABSTRACT

Sava, D., Hardage, B.A., DeAngelo, M. and Murray, P., 2011. Evaluating marine gas-hydrate systems. Part II: Rock-physics joint inversion of electrical resistivity and seismic velocities. *Journal of Seismic Exploration*, 20: 105-118.

The methodology for joint inversion presented in this paper uses a Bayesian approach, and combines rock-physics theories and empirical relations with stochastic simulations that were presented in Part I of this 2-paper series. We show examples of estimating gas-hydrate concentration and calculating the uncertainty associated with these estimates using electrical resistivity logs and 4C OBC seismic data across the Green Canyon area of the Gulf of Mexico. At calibration wells, we estimate hydrate concentration by jointly inverting electrical resistivity logs and seismic interval velocities.

KEY WORDS: gas hydrates, rock-physics, elastic properties, modeling, Gulf of Mexico.

INTRODUCTION

A method for joint inversion of electrical resistivity measurements and velocity data for estimating gas-hydrate concentration in deep-water environments is presented. The technique is based on a Bayesian (Bayes, 1783) approach and combines rock-physics elastic theories and empirical relations for electrical resistivity with stochastic simulations to account for the natural variability of the petrophysical parameters involved in the inversion.

0963-0651/11/$5.00

By combining electrical resistivity and seismic velocity, we can better constrain hydrate concentration and distribution within sediments, and we can reduce the inherent uncertainty associated with our predictions. This joint inversion method is especially critical for estimating hydrate concentration in deep-water near-seafloor strata because of the limited availability of well-log measurements. The typical well-log data across the hydrate stability zone are restricted to gamma-ray and electrical resistivity measurements, which cannot differentiate between different nonconductive phases in the pores, such as gas hydrate and free gas. On the other hand, P-wave velocity can distinguish between hydrates and free gas. However, usually there are no sonic logs available across the hydrate stability zone. Therefore, this method quantitatively combines seismic velocities and electrical resistivity logs at well locations to better constrain the hydrate concentration and distribution. The method is illustrated using examples from Green Canyon, Gulf of Mexico.

JOINT INVERSION OF ELECTRICAL RESISTIVITY AND VELOCITY WITH UNCERTAINTY ESTIMATION

In this section we present the rock-physics joint-inversion technique of electrical resistivity and seismic velocity for improved predictions on hydrate distribution and concentration. This method is based on the joint theoretical relation between hydrate concentration, resistivity, and velocity, derived using deterministic rock physics relations and stochastic simulations, as presented in Part I of this series (Sava and Hardage, 2010).

A typical inversion problem consists of three elements: 1) the *model parameters*, represented by the subsurface rock properties that we wish to detect and map (in this case, the hydrate concentration in the sediments), 2) the *data parameters* (e.g., seismic velocities and electrical resistivity measurements), and 3) the *physical laws* that relate the model parameters to the data parameters, which are given by *rock physics theories*, as discussed in Part I.

In applying our joint-inversion methodology, we account for the uncertainty of every parameter that enters into the calculation of hydrate concentration in our analytical models and also for the uncertainty related to measurement errors. The concepts of probability theory enable us to quantify this uncertainty and to combine quantitatively velocity and resistivity data into a joint inversion for hydrate concentration.

Our probabilistic approach allows us to account for the natural variability in the elastic properties of the mineral, hydrate, and fluid constituents of seafloor sediments, as well as for the variability in brine resistivity, cementation exponent, clay mineral resistivity, and other petrophysical parameters required

for our joint inversion of resistivity and seismic velocity to hydrate concentration.

To estimate hydrate concentration using seismic and resistivity data, we use a Bayesian approach (Bayes, 1783) formulated in the context of an inverse problem, as proposed by Tarantola (1987). First, we express our prior information about hydrate concentration (information obtained before analyzing any seismic or resistivity data) as a Probability Distribution Function (PDF). We denote this prior PDF as $\Lambda_M(C_{GH})$, where subscript M stands for "model" parameter, and C_{GH} is the gas hydrate concentration. In our study, this prior PDF is assumed to be a uniform distribution over all physically possible values for the hydrate pore-space fraction, meaning we allow this uniform distribution to range from 0 to 100-percent. (However, this method allows us to introduce into this prior PDF any additional information available from other sources).

Second, we combine this prior PDF of hydrate concentration, $\Lambda_M(C_{GH})$, with information provided by seismic and resistivity measurements at calibration wells. Our prior information and any information obtained from seismic and resistivity data are assumed to be statistically independent. This assumption allows the prior joint PDF that combines prior information on hydrate concentration and data, $\Lambda(C_{GH}, V_P, R)$, to be written as

$$\Lambda(C_{GH}, V_P, R) = \Lambda_M(C_{GH})\Lambda_D(V_P)\Lambda_D(R) \quad . \tag{1}$$

In eq. (1), subscript D stands for data and $\Lambda_D(V_P)$ and $\Lambda_D(R)$ are PDFs that account, respectively, for the observed mean values and measurement uncertainties in the seismic P-wave velocity data and electrical resistivity log data used in the hydrate inversion. We assume that these PDFs are Gaussian, with means given by the interval velocity values determined in the previous work by DeAngelo et al. (2008), and by the measured electrical resistivity values from the well log data. The standard deviations are assumed to be 5% of the mean values.

Third, we use Tarantola's (1987) strategy that states that the posterior PDF combining hydrate concentration and data, $\Psi(C_{GH}, V_P, R)$, is proportional to the prior joint PDF for hydrate concentration and data, $\Lambda(C_{GH}, V_P, R)$, multiplied by the joint theoretical PDF, $\xi(C_{GH},V_P,R)$, which we derive using stochastic rock physics modeling, as presented in Part I (Sava and Hardage, 2010). This theoretical PDF, $\xi(C_{GH}, V_P, R)$ is determined numerically as a smoothed normalized histogram, based on the multiple realizations for correlated pairs of C_{GH}, V_P, and R derived using rock physics elastic theory and Archie (1942) equation. Therefore, we can write at each depth-step:

$$\Psi(C_{GH}, V_P, R) = \Lambda(C_{GH}, V_P, R)\xi(C_{GH}, V_P, R) \quad . \tag{2}$$

From this posterior joint PDF, $\Psi(C_{GH}, V_P, R)$, we derive what is called the marginal distribution of hydrate concentration, $\Psi_M(C_{GH})$, by integrating the posterior joint PDF over velocity and resistivity data space. This marginal distribution, $\Psi_M(C_{GH})$, represents the posterior PDF for hydrate concentration in the pore space of the host sediment. From this posterior distribution we can derive the posterior expected value as our best estimate for hydrate concentration after combining the resistivity and seismic information using depth-calibrated rock physics theories. At the same time, we also have a measure of uncertainty associated with this estimate, given, for example, by the standard deviation of the posterior distribution on hydrate concentration.

INVERSION RESULTS

In this section we present results for estimating hydrate concentration at two well-locations in our study area in Green Canyon, Gulf of Mexico, where geotechnical borings and seafloor outcrops give hard evidence for the presence of gas hydrate. We choose two wells that have good logging coverage over the gas hydrate stability zone.

At each calibration well, we apply the Bayesian inversion procedure presented in the previous section to estimate the posterior PDF of hydrate concentration at each depth-step, using both local seismic velocity value and local resistivity-log data. This estimation utilizes the theoretical joint PDF, $\xi(C_{GH}, V_P, R)$ that we derive using the joint rock-physics stochastic modeling of electrical resistivity and seismic velocity, as presented in Part I.

Fig. 1 presents, on the left panel, the seismic P-wave interval velocities determined with a ray-trace-based velocity analysis technique at Well A. This method provides accurate P- and S-wave interval velocities (DeAngelo et al., 2008). The middle panel presents electrical resistivity, logged while drilling (LWD). The advantage of this LWD technique is that it provides electrical resistivity readings before any disturbances of the hydrate system can be caused by drilling, such as hydrate dissociation. On the left and middle panels we superimpose the baselines (c.f. Part I) for P-wave velocity and electrical resistivity of brine-saturated sediments (gray curves). We observe that both the seismic P-wave velocity and the electrical resistivity log show larger values than their corresponding baselines within the interval from 50 to 250 meters below the seafloor. This interval is interpreted to be hydrate-bearing because the presence of hydrates increases both the velocity and the electrical resistivity of their host sediments. We also observe that below this interval, the seismic P-wave velocity drops significantly below the baseline. This interval is interpreted as being charged with free gas because gas is known to lower the P-wave velocity significantly. Therefore, the base of hydrate stability zone (BHSZ) at this well is interpreted to be approximately 250 m below the seafloor,

as represented by the horizontal gray line in Fig. 1.

The electrical resistivity log, presented in the middle panel of the figure, shows resistivity higher than the baseline also below the BHSZ. This response is present because free gas and hydrates are both non-conductive phases, and an electrical resistivity log cannot differentiate between these two resistive components. However, P-wave velocity can distinguish between hydrate and free gas. Therefore, combining seismic information with electrical resistivity measurements helps reduce the ambiguity about hydrate distribution within sub-seafloor sediments.

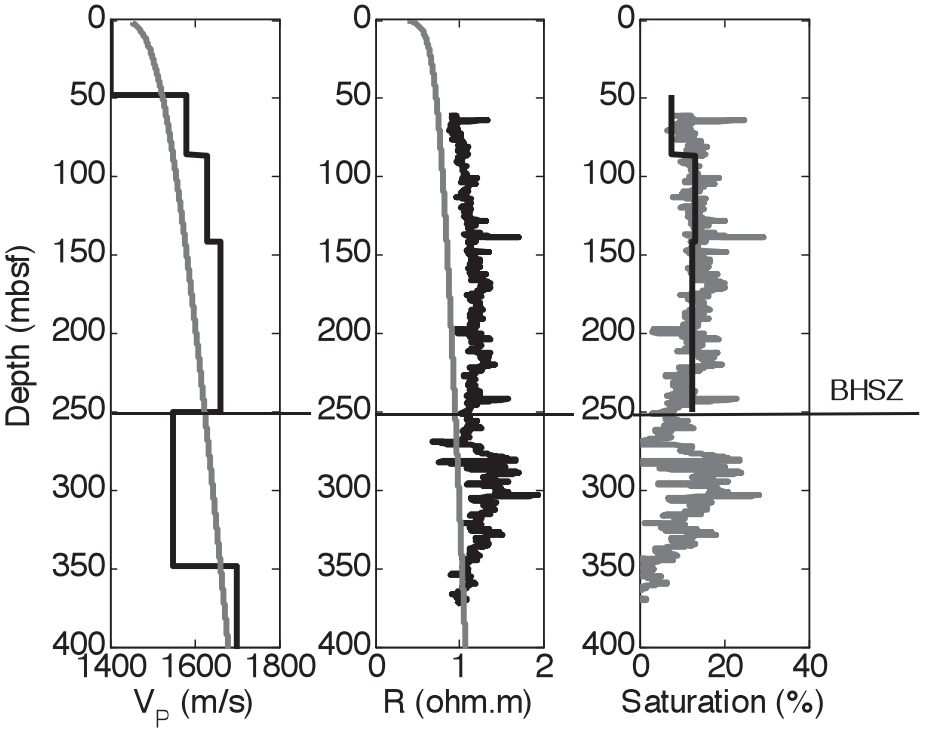

Fig. 1. Well A - Seismic P-wave interval velocities (left panel) and electrical resistivity log (middle panel) with their corresponding baseline for brine-saturated sediments (gray curves). The posterior expected value for saturation of the non-conductive phase (either hydrate or free gas) determined from electrical resistivity log data is shown as the gray curve on the right panel. Superimposed on the right panel are the expected values for hydrate concentration, based on the P-wave interval velocities alone, across the gas-hydrate stability zone.

The third panel in Fig. 1 presents the posterior expected value (gray curve) for the saturation of the non-conductive phase, be that phase hydrate or free gas. This posterior expected values are derived from the posterior PDF $\Psi(C_{GH}, V_P)$, using electrical resistivity data alone in eq. (2). Superimposed on the same panel (black curve) is the expected estimate for hydrate concentration determined independently from the posterior PDF $\Psi(C_{GH}, V_P)$ in eq. (2), using only seismic P-wave interval velocities between 50 m to 250 m below the seafloor. These estimates assume that the hydrates are disseminated and load-bearing within those intervals (Sava and Hardage, 2006). We observe a good agreement between the estimates for hydrate concentration determined from electrical resistivity log and independently from the P-wave velocity. This agreement confirms that a good calibration was determined for the parameters that enter into both the Archie (1942) equation and the rock physics elastic model. It also allows us to conclude that the assumption of load-bearing hydrates may be representative of the real-earth hydrates at this location.

Seismic interval velocities have significantly lower resolution than the electrical resistivity logs. Therefore, for our joint inversion procedure, we use the average value for resistivity over each seismic velocity interval. Detailed information about hydrate concentration can be obtained at each well based on electrical resistivity inversion alone.

Fig. 2 presents the posterior probability distribution functions $\Psi_M(C_{GH})$ for gas hydrate concentration in Well A for the following three intervals within the gas hydrate stability zone: 1) between 50 and 80 meters (upper panel), 2) between 80 and 140 meters (middle panel), and 3) between 140 and 250 meters (lower panel). The dashed dark gray curves correspond to the posterior PDFs obtained from resistivity log inversion (assuming an average value for resistivity log over the specified intervals). The posterior expected values for hydrate concentration derived from electrical resistivity measurements for each of the three intervals are: 11.1% for the upper interval from 50 meters to 80 meters, 14% for the middle interval from 80 meters to 140 meters, and 13.6% for the interval between 140 meters to 250 meters below the seafloor. Their corresponding standard deviations are 3.7%, 3.4%, and 3.7%, respectively.

The dotted lighter gray curves correspond to the posterior PDFs obtained from seismic P-wave velocity inversion alone. The posterior expected values for hydrate concentration derived from seismic P-wave velocities in each interval are: 7.3% for the upper interval, 12.6% for the middle interval, and 12.1% for the lower interval. Their corresponding standard deviations are slightly larger than the ones associated with the hydrate concentration predictions derived from electrical resistivity log, and have the following values: 4.1%, 4.3%, and 4.4%.

The black solid curves correspond to the posterior PDFs $\Psi(C_{GH}, V_P, R)$, from the joint inversion of resistivity and seismic P-wave interval velocity, using

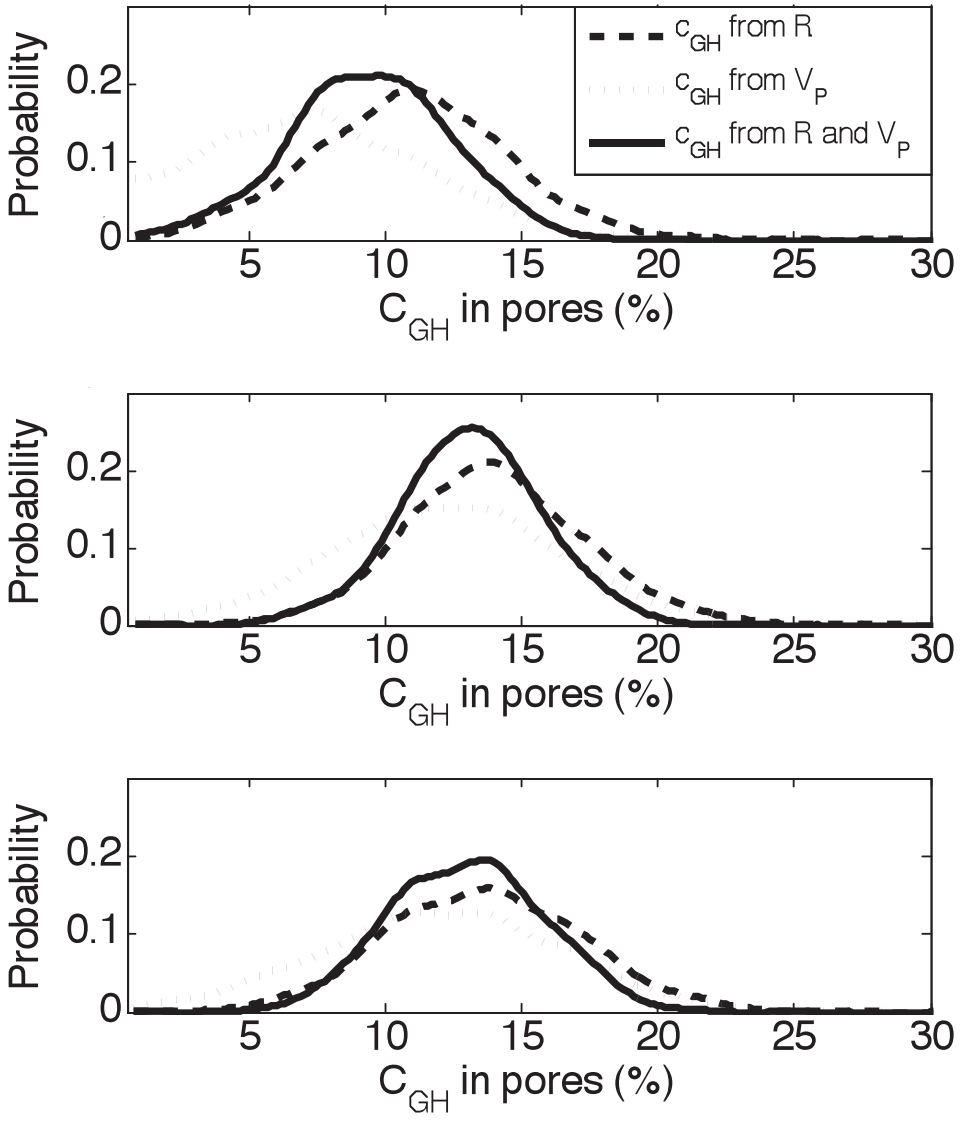

Fig. 2. Well A - Posterior PDFs $\Psi_M(C_{GH})$ for gas hydrate concentration for the three velocity intervals between 50-80 m (upper panel), 80-140 m (middle panel), and 140-250 m (lower panel) from Well A (Fig. 5). The dashed darker gray curves correspond to the posterior PDFs from resistivity log inversion (assuming an average value for resistivity log over each seismic P-wave intervals). The dotted lighter gray curves correspond to the posterior PDFs from the seismic P-wave velocity inversion. The black solid curves correspond to the posterior PDFs of the joint inversion of the blocked resistivity and seismic interval velocity.

eq. (2). The posterior expected values derived from these posterior joint PDFs indicate hydrate concentration expected values in the pores in each of the three intervals, 9.4% in the upper interval, 13.3% in the middle interval, and 12.9% in the lower interval. The standard deviations, which represent a measure of uncertainty associated with these joint predictions for each interval, are: 2.9%, 2.7%, and 2.8%, respectively. As expected, we find that the uncertainty associated with hydrate concentration is reduced when a joint inversion is done using both velocity and resistivity data, compared to the uncertainty that is obtained when using velocity or resistivity information alone. The results for the posterior expected values for hydrate concentration and their associated standard deviations for each of the intervals from Well A are summarized in Table 1.

Table 1. Results for the posterior expected values (mean) and the associated standard deviation (std.) for hydrate concentration in sediment pores (C_{GH}) for the three seismic interval velocities within the hydrate stability zone from Well A, estimated from resistivity (R), P-wave velocity (V_P), and from the joint inversion of resistivity and P-wave velocity (R and V_P).

WELL A	C_{GH} from R		C_{GH} from V_P		C_{GH} from R and V_P	
Seismic intervals	mean (%)	std. (%)	mean (%)	std. (%)	mean (%)	std. (%)
50 - 80 m	11.1	3.7	7.3	4.1	9.4	3.0
80 - 140 m	14.0	3.4	12.6	4.3	13.3	2.7
140 - 250 m	13.6	3.7	12.1	4.4	13	2.9

We performed the same analysis at a different well location, Well B. (Fig.3). The left panel presents the seismic P-wave interval velocity, while the middle panel presents the electrical resistivity log. On each of these panels we superimpose the corresponding baselines for P-wave velocity and electrical resistivity of brine-saturated sediments (gray curves).

From Fig. 3 we observe again that both the seismic P-wave velocity and the electrical resistivity log have values larger than their corresponding baselines within an interval from 80 to 210 meters below seafloor. This interval is interpreted to be hydrate-bearing. We again observe that below this interval, the seismic P-wave velocity drops below the computed baseline for 100% brine-saturated sediments, as it did in the case for Well A, presented in Fig. 1. This interval is again interpreted to contain free gas. The base of the hydrate stability zone (BHSZ) at this well is interpreted to be approximately 210 meters below seafloor and is represented by the horizontal gray line in Fig. 3. The electrical resistivity log in the middle panel shows again that resistivity exceeds the

baseline because of the presence of free gas. This resistive interval could be mistaken as being hydrate bearing if only resistivity data are used to define a BHSZ horizon. The right panel in Fig. 3 presents the posterior expected value (gray curve) for the saturation of the non-conductive phase (either hydrate or free gas) determined from the electrical resistivity log.

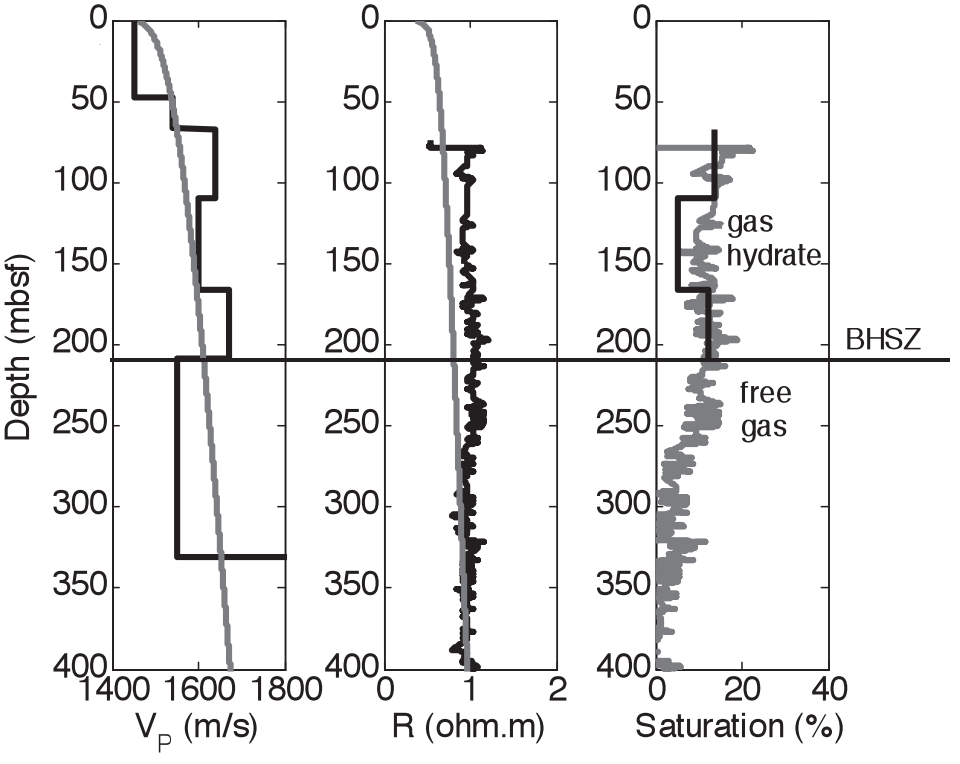

Fig. 3. Well B - Seismic interval P-wave velocities (left panel) and electrical resistivity log (middle panel) with their corresponding baselines for brine-saturated sediments (gray curves). The posterior expected value for the saturation of the non-conductive phase (either hydrate or free gas) from the electrical resistivity log is shown as the gray curve on the right panel. Superimposed on the right panel are the expected values for hydrate concentration, based on the P-wave interval velocities alone, across the gas-hydrate stability zone.

We again superimpose on the panel the posterior estimates for hydrate concentration determined independently from the seismic P-wave interval velocities within the sediments from 80 to 210 meters below the seafloor. We observe a good agreement between the estimations for hydrate concentration determined from electrical resistivity log data and from P-wave velocity for the

upper interval from 80 to 110 meters and for the lower interval from 165 to 210 meters, with a discrepancy for the middle interval from 110 to 165 meters. The hydrate estimation from velocity is lower than the estimation from resistivity in this interval. There are various factors that can contribute to this discrepancy, such as changes in mineralogy, pore fluids, effective pressure, and hydrate morphology. If some hydrates are floating in the pores, without fully contributing to the load-bearing frame of the sediments, the increase in velocity would not be as large as predicted by our modeling. Therefore, the assumption of load-bearing hydrates can yield smaller estimates for hydrate concentration if in reality some hydrate clathrates are floating in the porous space and are only partly contributing to supporting the shear load.

Fig. 4 presents the posterior probability distribution functions $\Psi_M(C_{GH})$ for gas hydrate concentration in Well B for the three P-wave velocity intervals: 1) between 80 and 110 meters (upper panel), 2) between 110 and 165 meters (middle panel), and 3) between 165 and 110 meters (lower panel). The dashed dark gray curves correspond to the posterior PDFs obtained from resistivity log inversion (assuming an average value for the resistivity log over the specified intervals). The posterior expected values for hydrate concentration derived from electrical resistivity measurements for each of the three intervals are: 13.1% for the upper interval, 10.3% for the middle interval, and 13% for the lower interval between 165 to 210 meters below seafloor. Their corresponding standard deviations are 4%, 3.7%, and 3.7%, respectively. The dotted lighter gray curves correspond to the posterior PDFs obtained from seismic P-wave velocity inversion alone. The posterior expected values for hydrate concentration derived from seismic P-wave velocities in each interval are: 12.8% for the upper interval, 5.8% for the middle interval, and 12.5% for the lower interval. Again, their corresponding standard deviations are slightly larger than the ones associated with the hydrate concentration predictions based on electrical resistivity, and they have the following values: 4.4%, 3.9%, and 4.4%.

The black solid curves correspond to the posterior PDFs from the joint inversion of resistivity and seismic P-wave interval velocity. The posterior expected values derived from these posterior joint PDFs indicate expected values for hydrate concentration in the pores in each of the three intervals as 13.1% in the upper interval, 8% in the middle interval, and 12.7% in the lower interval. The standard deviations, which represent a measure of uncertainty associated with these joint predictions for each intervals are: 3.1%, 2.9%, and 3%,respectively. As expected, we find again that the uncertainty associated with hydrate concentration reduces when a joint inversion is performed using both velocity and resistivity data, compared to the uncertainty that is obtained when using velocity or resistivity information alone. The results for the posterior expected values for hydrate concentration and their associated standard deviations for each of the intervals considered in Well B are summarized in Table 2.

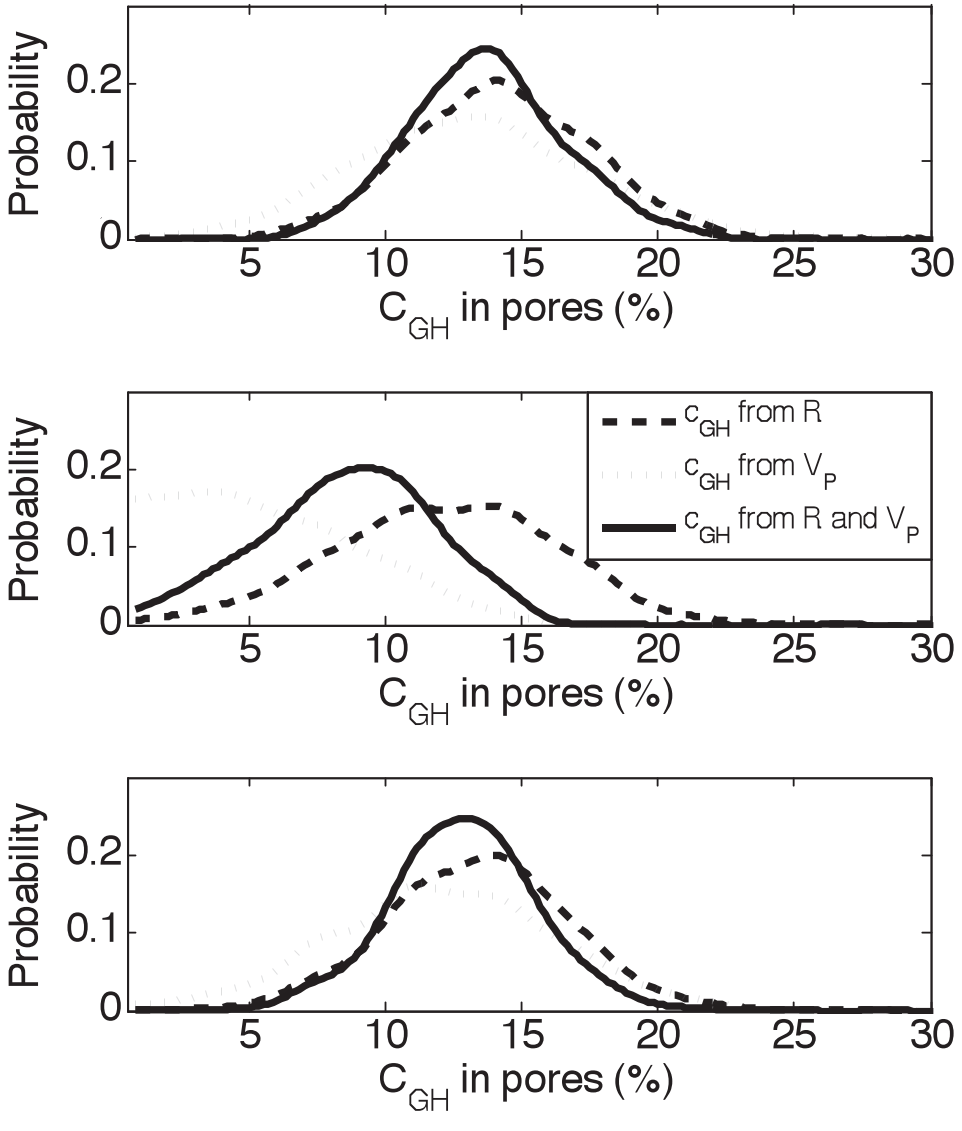

Fig. 4. Well B- Posterior PDFs $\Psi_M(C_{GH})$ for gas hydrate concentration for the three velocity intervals between 80-110 m (upper panel), 110-165 m (middle panel), and 165-210 m (lower panel) from Well B (Fig. 3). The dashed darker gray curves correspond to the posterior PDFs from resistivity log inversion (assuming an average value for resistivity log over each seismic P-wave intervals). The dotted lighter gray curves correspond to the posterior PDFs from the seismic P-wave velocity inversion. The black solid curves correspond to the posterior PDFs of the joint inversion of the blocked resistivity and seismic interval velocity.

Table 2. Results for the posterior expected values (mean) and the associated standard deviation (std.) for hydrate concentration in sediment pores (C_{GH}) for the three seismic interval velocities within the hydrate stability zone from Well B, estimated from resistivity (R), P-wave velocity (V_P), and from the joint inversion of resistivity and P-wave velocity (R and V_P).

WELL B	C_{GH} from R		C_{GH} from V_P		C_{GH} from R and V_P	
Seismic intervals	mean (%)	std. (%)	mean (%)	std. (%)	mean (%)	std. (%)
80 - 110 m	13.1	4	12.8	4.4	13.1	3.1
110 - 165 m	10.3	3.7	5.8	3.9	8	2.9
165 - 210 m	13	3.7	12.5	4.4	12.7	3

By comparing Well A and Well B we observe the same qualitative response of the electrical resistivity and seismic velocity over the zone of interest. At both well locations we can identify intervals of higher seismic P-wave velocity and electrical resistivity values than their corresponding baselines, within a zone interpreted as hydrate-bearing sediments. Below these intervals there is a decrease in the seismic P-wave velocities, which drop below the computed baselines for 100% brine-saturated sediments at both well locations. The decrease in P-wave velocities is interpreted to be due to the presence of free gas. However, the electrical resistivity logs show the resistivity exceeding the baseline both in the higher and lower seismic interval velocities, because electrical resistivity cannot differentiate between the non-conductive hydrate or free gas in the sediment pores.

The independent estimates of hydrate concentration from resistivity and velocity are in good agreement at both well locations, supporting the assumption of load-bearing hydrates at these wells. It would have been ideal to compare the results obtained here with direct measurements of hydrate concentration in these wells. However, coring and preserving the cores to prevent hydrate dissociation for further measurements and analysis in lab is not performed on a regular basis, and most hydrate studies rely on remote measurements. The advantage of using remote measurements for hydrate characterization, such as seismic data, is that they allow us to make predictions about hydrate presence and concentration before drilling. These studies help us avoid possible hazardous conditions that can occur due to hydrate dissociation.

CONCLUSIONS

Gas hydrate distribution and concentration from sediments in deep-water, near-seafloor strata can be estimated based on a joint inversion methodology of electrical resistivity and P-wave velocity. This technique uses a Bayesian approach and combines rock-physics elastic theories and empirical relations for electrical resistivity with stochastic simulations. All of the parameters involved in relating hydrate concentration to electrical resistivity and velocity are expressed as probability distribution functions, which vary with depth below the seafloor. The probabilistic approach allows us to incorporate the inherent uncertainties associated with each model and data parameter. Therefore, using this method we account for the natural variability in the elastic properties of the mineral, hydrate, and fluid constituents of near-seafloor sediments, as well as for the variability in brine resistivity, cementation exponent, clay mineral resistivity, and all other petrophysical parameters required for our joint inversion of resistivity and seismic velocity to hydrate concentration. At the same time, this technique allows us to estimate the uncertainty associated with the final results for hydrate concentration. By combining electrical resistivity measurements with seismic velocity we can better constrain hydrate concentration and distribution within sediments, and reduce the uncertainty associated with our predictions.

This quantitative integration of electrical resistivity and P-wave velocity is critical for estimating hydrate concentration in deep-water near-seafloor strata because well-log data across hydrate stability zones in conventional oil and gas wells are limited to gamma-ray and electrical resistivity measurements, which cannot differentiate between nonconductive gas hydrate and free gas in pores. In contrast, P-wave velocity can distinguish between hydrates and free gas. Our joint inversion method allowed us to quantitatively combine seismic velocities and the electrical resistivity logs at well locations to better constrain the hydrate concentration and distribution.

Based on the examples from Green Canyon presented in the paper, we concluded that a careful calibration of both electrical and elastic properties of sediments from deep-water, near-seafloor strata can yield similar results for hydrate concentration estimated independently from electrical resistivity and from seismic velocity. The agreement between the independent estimates of hydrate concentration at well locations confirms the validity of a load-bearing-hydrate assumption in marine sediments. Slightly lower estimates of hydrate concentration were estimated from velocity than from electrical resistivity in some intervals, which can be partly explained if some hydrates are floating in the pores without fully contributing to the load-bearing frame of the sediments.

The good agreement between independent estimates of hydrate concentration from electrical resistivity and from seismic velocity measured at

calibration wells will allow us to make predictions of hydrate concentration based on seismic information alone away from the wells.

The joint inversion technique presented in this paper enabled us to make more reliable and better constrained predictions about hydrate concentration and distribution, and to quantify the associated uncertainty, in the context of scarce availability of well-log data that seems to always be encountered in studying deep-water hydrate systems.

ACKNOWLEDGEMENTS

Research funding was provided by the U.S. Department of Energy (DOE/NETL Contract DE-PS26-05NT42405) and by the Minerals Management Service (Contract MMS 0105CT39388). We would like to thank Leon Thomsen for his excellent input in the reviewing of the manuscript. This work was published with the approval of the director of the Bureau of Economic Geology.

REFERENCES

Archie, G.E., 1942. The electric resistivity log as an aid in determining some reservoir characteristics. Transact. AIME, 46: 54.

Bayes, T., 1783. An essay towards solving a problem in the doctrine of chances. Phil. Transact. Roy. Soc., 53: 370-418.

DeAngelo, M.V., Murray, P.E., Hardage, B.A. and Remington, R.L., 2008. Integrated 2D 4-C OBC seismic velocity analysis of near-seafloor sediments, Green Canyon, Gulf of Mexico. Geophysics, 73: 109-115.

Sava, D.C. and Hardage, B.A., 2006. Rock physics characterization of hydrate-bearing deepwater sediments. The Leading Edge, 25: 616-619.

Sava, D.C. and Hardage, B.A., 2010. Evaluating marine gas-hydrate systems, Part I: Stochastic rock-physics models for electrical resistivity and seismic velocities of hydrate-bearing sediments. J. Seismic Explor., 19: 371-386.

Tarantola, A., 1987. Inverse Problem Theory. Elsevier Science Publishers, Amsterdam.